Doping effect of nano-diamond on superconductivity and flux pinning in MgB_2

C H Cheng[1]**, H Zhang**[1,2]**, Y Zhao**[1,2,3]**, Y Feng**[4]**, X F Rui**[2]**,
P Munroe**[1]**, H M Zeng**[5]**, N Koshizuka**[6] **and M Murakami**[6]

[1] School of Materials Science and Engineering, University of New South Wales,
Sydney 2052, NSW, Australia
[2] State Key Lab for Mesophysics, Department of Physics, Peking University, Beijing 100871,
People's Republic of China
[3] Superconductivity R&D Center, Mail Stop 152#, Southwest Jiaotong University, Chengdu,
Sichuan 610031, People's Republic of China
[4] Northwest Institute for Nonferrous Metal Research, PO Box 51, Xi'an, Shaanxi 710016,
People's Republic of China
[5] Key Laboratory of Polymeric Composites and Functional Materials, The Ministry of
Education, Zhongshan University, Guangzhou 510275, People's Republic of China
[6] Superconductivity Research Laboratory, ISTEC, 1-10-13 Shinonome, Koto-ku,
Tokyo 135-0062, Japan

E-mail: c.cheng@unsw.edu.au

Abstract

Doping effect of diamond nanoparticles on the superconducting properties
of MgB_2 bulk material has been studied. It is found that the superconducting
transition temperature T_c of MgB_2 is suppressed by the diamond doping,
however, the irreversibility field H_{irr} and the critical current density J_c are
systematically enhanced. Microstructural analysis shows that the
diamond-doped MgB_2 superconductor consists of tightly-packed MgB_2
nano-grains ($\sim$50–100 nm) with highly-dispersed and uniformly-distributed
diamond nanoparticles ($\sim$10–20 nm) inside the grains. High density of
dislocations and diamond nanoparticles may take the responsibility for the
enhanced flux pinning in the diamond-doped MgB_2.

1. Introduction

Since the discovery of superconductivity at 39 K in MgB_2
[1], significant progress has been made in improving the
performance of MgB_2 materials [2–7]. MgB_2 offers the
possibility of wide engineering applications in the temperature
range 20–30 K, where conventional superconductors, such as
Nb_3Sn and Nb–Ti alloy, cannot play any roles due to their low
T_c. However, the realization of large-scale applications for
MgB_2-based superconductivity technology essentially relies
on the improvement of the pinning behaviour of MgB_2 in
high fields. As it has poor grain connection and a lack
of pinning centres, MgB_2 often exhibits a rapid decrease in
critical current density, J_c, in high magnetic fields. Fortunately,
through the formation of nanoparticle structures in bulk

MgB_2 [3–5] and thin films [7], the problem of the poor grain
connection can be solved, and the flux pinning force can
also be significantly enhanced due to an increase of pinning
centres served by grain boundaries. In order to improve
further the performance of MgB_2, it is necessary to introduce
more pinning centres, especially those consisting of nano-sized
second-phase inclusions which often provide strong pinning
forces.

Nano-diamond, prepared by the detonation technique, has
been widely used as an additive to improve the performance
of various materials [8]. However, nano-diamond-doping
effect on the superconducting properties MgB_2 has never
been reported although carbon with other forms has been
used as dopants in MgB_2 [9–11]. The high dispersibility of
the nano-diamond powder makes it possible to form a high

density of nano-inclusions in MgB_2 matrix. In this paper, we have investigated the doping effect of nano-diamond on the superconducting properties of MgB_2. Our results show that the nano-diamond-doped MgB_2 consists of tightly-packed MgB_2 nano-grains ($\sim$50–100 nm) with diamond nanoparticles ($\sim$10–20 nm) wrapped within the grains. This unique microstructure provides the samples with a good grain connection for the MgB_2 phase and a high density of flux-pinning centres served by the diamond nanoparticles. Compared to the MgB_2 bulk materials doped with other nanoparticles [3–7], the irreversibility line has been significantly improved and the J_c in high magnetic fields has been largely increased in these nano-diamond-doped MgB_2.

2. Experimental details

The MgB_2–diamond nano-composites with compositions of $MgB_{2-x}C_x$ ($x = 0\%, 5\%, 8\%$ and 10%) were prepared by solid-state reaction at ambient pressure. Mg powder (99% purity, 325 meshes), amorphous B powder (99% purity, submicron size) and nano-diamond powder (10–20 nm) were mixed and ground in air for 1 h. An extra 2% of Mg powder was added in the starting materials to compensate the loss of Mg caused by high-temperature evaporation. The mixed powders were pressed into pellets with dimensions of $20 \times 10 \times 3$ mm^3 under a pressure of 800 kg cm^{-2}, sandwiched into two MgO plates, sintered in flowing Ar at 800 °C for 2 h, and then quenched to room temperature in air. In order to compare the substitution effect of carbon in boron in MgB_2 with the additional effect of the nano-diamond in MgB_2, a sample with an added 1.5 wt% of nano-diamond in MgB_2 was prepared. The sintering temperature and the sintering time for this sample were reduced respectively to 730 °C and 30 min in order to reduce the chemical reaction between the MgB_2 and the diamond. This sample has been referred to as '1.5 wt% C'.

The crystal structure was investigated by powder x-ray diffraction (XRD) using an X'pert MRD diffractometer with Cu Kα radiation. The microstructure was analysed with a Philips CM200 field emission gun transmission electron microscope (FEGTEM). DC magnetization measurements were performed in a superconducting quantum interference device (SQUID, Quantum Design MPMS-7). J_c values were deduced from hysteresis loops using the Bean model. The values of the irreversibility field, H_{irr}, were determined from the closure of hysteresis loops with a criterion of 10^2 A cm^{-2}.

3. Results and discussion

Figure 1 shows the XRD patterns of the nano-diamond powder and the typical MgB_2–diamond composites. The reflection (111) of the diamond is extremely broad and an amorphous-phase-like background can be seen in the XRD pattern. The particle size of the nano-diamond powder is estimated to be about 20 nm according to the width of the reflection. In relation to the nano-diamond-doped MgB_2, one of the impurity phases is MgO, which may have formed during the mixing of raw materials in air. Diamond should be present as another impurity phase in the composites; however, its main reflection (111) cannot be seen in XRD patterns, due to an overlap with the MgB_2 (101) peak. With increasing
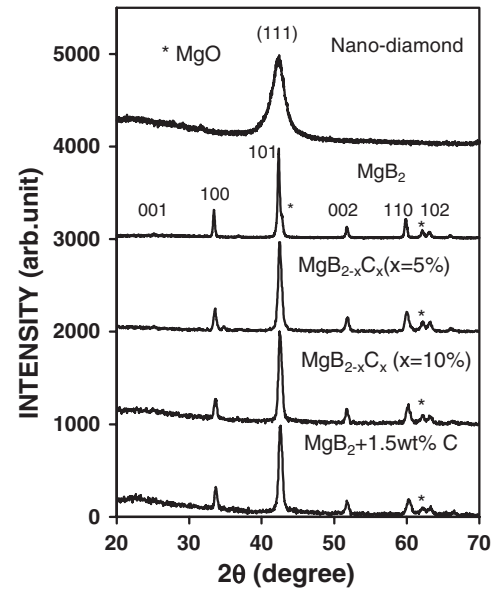
Figure 1. Powder XRD patterns for nano-diamond-doped MgB_2. The pattern on the top row is for the nano-diamond.
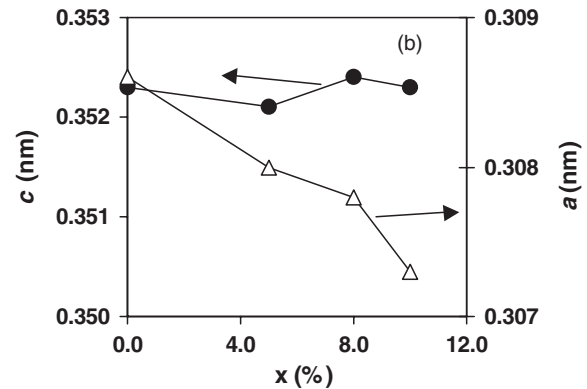

Figure 2. Doping dependence of lattice constants for nano-diamond-doped MgB_2.

doping level, an amorphous-phase-like background in the XRD pattern gradually appears, suggesting the existence of unreacted nano-diamond in the sample. As for the diamond-added MgB_2 sample (1.5 wt% C), which contains an $x = 5.4\%$ equivalent percentage of carbon atoms, the background of its XRD pattern shows some similarity to the background of the nano-diamond, suggesting that a substantial amount of unreacted nano-diamond exists within this sample.

Figure 2 shows the doping-level dependence of the lattice constants for the nano-diamond-doped MgB_2. The length of c-axis does not exhibit significant change with increasing nano-diamond doping level, but the a-axis is systematically decreased by doping the nano-diamond, indicating that a certain amount of carbon atoms have substituted for boron atoms in MgB_2. This result is consistent with those reported by other groups, which shows that partial substitution of boron by carbon results in a decrease of the lattice parameter [9–11].

Figure 3 shows the temperature dependence of magnetization at 2 mT for nano-diamond-doped MgB_2. The superconducting transition temperature T_c decreases with increasing doping level. This result is consistent with those reported by other groups on the carbon-doped MgB_2, which
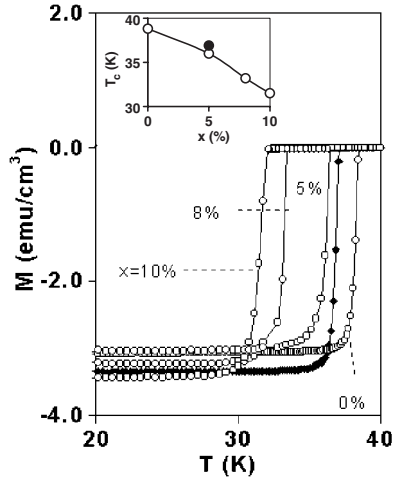
Figure 3. Temperature dependence of magnetization at 2 mT for nano-diamond-doped MgB_2. Inset: doping-level dependence of T_c. The closed circles represent the results for the sample 1.5 wt% C in both the main and the inset figures.

suggests that carbon can partially substitute boron in MgB_2, decrease the carrier (hole) concentration and consequently decrease the T_c [9, 10]. The doping-level dependence of T_c is shown in the inset of figure 3. The values of onset T_c for these carbon-substituted MgB_2 samples are 38.6 K for $x = 0\%$, 36.1 K for $x = 5\%$, 33.0 K for $x = 8\%$ and 31.3 K for $x = 10\%$ (see the open circles). The T_c for the sample 1.5 wt% C is 36.9 K (see the closed circle), which is higher than that for the sample of $x = 5\%$ ($T_c = 36.1$ K), despite the former having a higher equivalent atomic percentage of carbon ($x = 5.4\%$). This result suggests that only a part of carbon have been doped into the crystal structure of MgB_2 in the diamond-added sample, consistent with the XRD analysis.

Figure 4 shows the magnetic field dependence of J_c at 10, 20 and 30 K for the carbon-substituted MgB_2 samples. At 30 K, the undoped MgB_2 exhibits the highest J_c and the slowest decrease of J_c with H; whereas the sample of $x = 10\%$ shows the lowest J_c and the quickest drop of J_c with H. It is evident that the J_c–H behaviour at 30 K for these samples is positively correlated to their T_c values. However, when the temperature decreases to the values far below T_c, a totally different situation appears. For example, at 10 and 20 K, the diamond-doped samples show a much better J_c–H behaviour. The J_c drops much more slowly in diamond-doped samples than in pure MgB_2. The best J_c at 20 K is found in the sample of $x = 10\%$, reaching a value of 6×10^3 A cm^{-2} in a 4 T field, indicating that a strong flux pinning force exists in these diamond-doped samples.

However, the effect of diamond doping on the enhancement of flux pinning in MgB_2 may be counterbalanced by its suppression on superconductivity, as clearly shown in the situation of $T = 30$ K (see figure 3). This counterbalancing effect may also exist at other temperatures, even when the effect of the J_c-enhancement is dominant. The further increase of J_c depends critically on reducing the T_c-suppression effect in the MgB_2–diamond composite. This idea is confirmed by the results obtained in the diamond-added sample, 1.5 wt% C, which has a higher T_c than other diamond-doped samples (see figure 3) and contains more nano-diamond inclusions as suggested by the XRD analysis (see figure 1) and confirmed
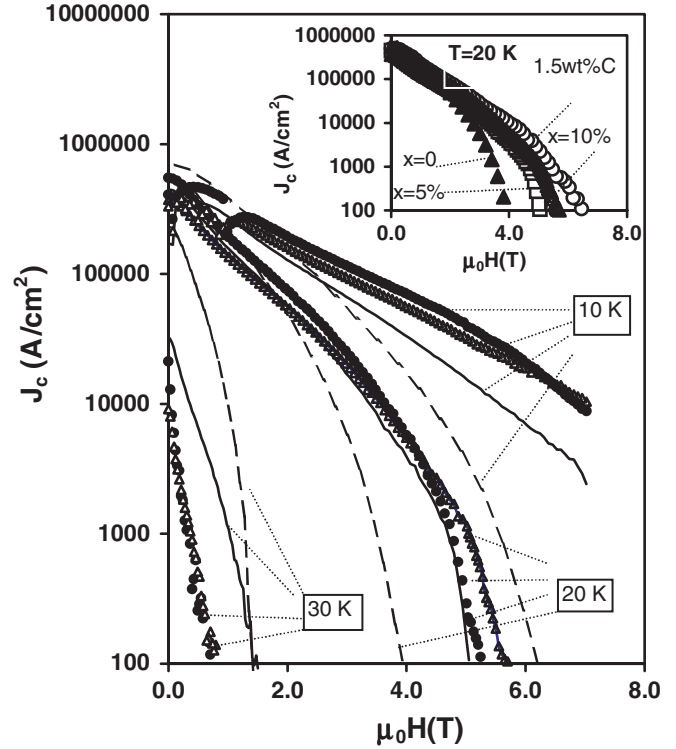

Figure 4. Magnetic field dependence of J_c at 10, 20 and 30 K for nano-diamond substituted MgB_2 with $x = 0\%$ (dashed lines), 5% (solid lines), 8% (solid circles) and 10% (opened triangles). Inset: comparison of J_c–H behaviour at 20 K between the diamond-added sample (1.5 wt% C) with some diamond-substituted samples ($x = 0\%$, 5% and 10%).

by our TEM analysis shown below. As shown in the inset of figure 4, the diamond-added sample shows a much better J_c–H behaviour than the carbon-substituted sample. Its J_c reaches 1×10^4 A cm^{-2} at 20 K and 4 T, and its H_{irr} reaches 6.4 T at 20 K. In fact, at all temperatures below 35 K, the J_c–H behaviour (results at 20 K are shown here only) of the diamond-added sample are much better than those of other samples in this study.

The H_{irr}–T relations for the diamond-doped MgB_2 are shown in figure 5. The H_{irr} (T) curves get steeper with increasing doping level, although the substitution of carbon for boron decreases the superconducting transition temperature. The best value of H_{irr} for these diamond-substituted MgB_2 samples including $x = 0\%$, 5%, 8% and 10% is found in the sample with $x = 10\%$, reaching 5.7 T at 20 K. However, the diamond-added MgB_2 (1.5 wt% C) shows a better H_{irr}–T behaviour than the diamond-substituted MgB_2. The H_{irr} value reaches 6.3 T at 20 K. The result clearly shows that the diamond doping does enhance the flux pinning in MgB_2 significantly, and also suggests that the pinning behaviour of the nano-diamond-doped MgB_2 depends on the density of the unreacted diamond nanoparticles in the samples.

Figure 6 shows the typical results from microstructural analysis for the diamond-substituted MgB_2 (figure 6(a)) and diamond-added MgB_2 samples (figure 6(b)). The diamond-substitutional sample mainly consists of relatively large MgB_2 grains ($\sim 1~\mu m$ or so in size) with a high density of dislocations. In some areas, discrete nano-sized particles can be seen. The diamond-added sample mainly consists of two kinds
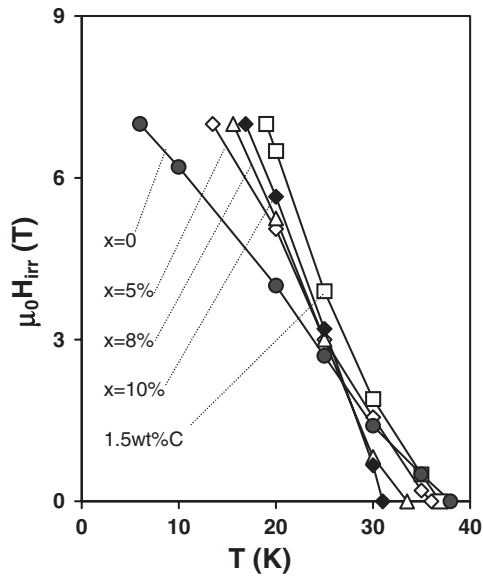
Figure 5. Variation of H_{irr} with temperature T for nano-diamond-doped MgB$_2$.
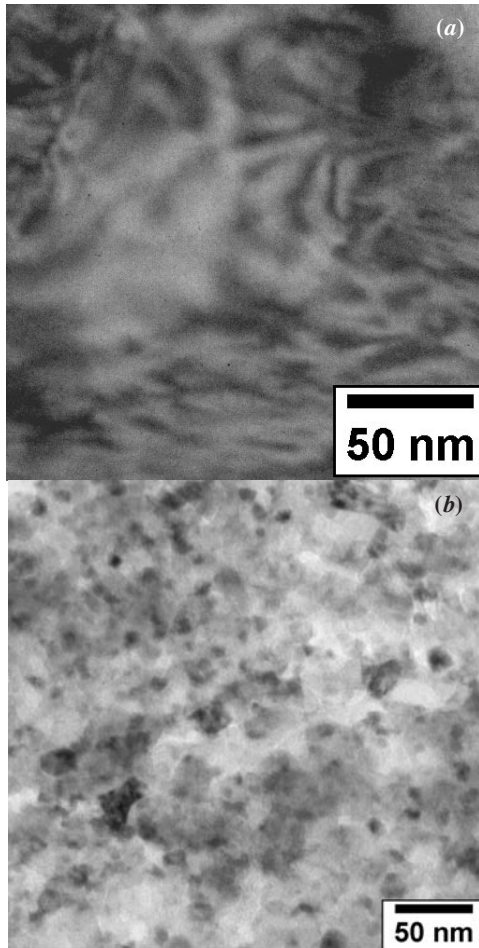
Figure 6. FEGTEM micrographs for (*a*) diamond-substituted MgB$_2$ with $x = 5\%$; (*b*) diamond-added MgB$_2$ with the carbon content of 1.5 wt%. The atomic percentages of carbon in the sample 1.5 wt% C is equivalent to $x = 5.4\%$.

of nanoparticles: MgB$_2$ grains with a size of 50–100 nm and diamond particles with a size of 10–20 nm. In fact, this diamond-added MgB$_2$ forms a typical nano-composite

material. The nano-diamond particles are inserted into the MgB$_2$ grains. As the *ab*-plane coherence length of MgB$_2$ is about 6–7 nm [12], these 10- to 20-nm-sized diamond inclusions, with a high density, are ideal flux pinning centres and are responsible for the high performance in our samples.

It is worth noting that the enhancement of flux pinning in nano-diamond-doped MgB$_2$ is even better than the Ti-doped MgB$_2$ [3–5], where the TiB$_2$ nanoparticles mainly stay in grain boundaries, which results in a J_c of 9×10^4 A cm^{-2} at 2 T and a H_{irr} of 4.6 T at 20 K (for a comparison, the corresponding values for the present system are J_c (20 K, 2 T) $= 1.1 \times 10^5$ A cm^{-2} and H_{irr} (20 K) $= 6.3$ T). This suggests that a highly-dispersed distribution of nano-inclusions in MgB$_2$ is more effective in enhancing flux pinning than a more localized distribution in the grain boundaries. Besides, compared to the Y$_2$O$_3$ nanoparticle doping which results in a J_c (20 K, 2 T) $= 8 \times 10^4$ A cm^{-2} and H_{irr} (20 K) $= 5.5$ T, an advantage of the nano-diamond doping is that the lattice contact of the cubic diamond ($a = 0.356$ nm) is very close to the *c*-axis of MgB$_2$ ($c = 0.352$ nm). Therefore, these diamond nanoparticles may provide nucleation centres for MgB$_2$ and are tightly bound to them. This may explain why our MgB$_2$–diamond nano-composite performs much better than the nano-Y$_2$O$_3$-doped MgB$_2$ [6]. It is expected that the performance of the MgB$_2$–diamond nano-composite may be further improved by optimizing the microstructure and the doping levels.

4. Summary and conclusions

In summary, we have investigated the doping effect of diamond nanoparticles on the superconducting properties of MgB$_2$ bulk material. We have observed that the superconducting transition temperature T_c of MgB$_2$ is suppressed by the diamond-doping, such as doping with other forms of carbon. However, the irreversibility field H_{irr} and the critical current density J_c are systematically enhanced by doping nano-diamond. Microstructural analysis shows that the diamond-doped MgB$_2$ superconductor consists of tightly-packed MgB$_2$ nano-grains ($\sim$50–100 nm) with highly-dispersed and uniformly-distributed diamond nanoparticles ($\sim$10–20 nm) inside the grains. High density of dislocations and diamond nanoparticles may be responsible for the enhancement of the flux pinning in the nano-diamond-doped MgB$_2$.

Acknowledgments

References

[1] Nagamatsu J, Nakagawa N, Muranaka T, Zenitani Y and Akimitsu J 2001 *Nature* **410** 63
[2] Cheng C H, Zhao Y, Feng Y, Zhu X T, Koshizuka N and Murakami M 2003 *Supercond. Sci. Technol.* **16** 125

[3] Zhao Y, Feng Y, Cheng C H, Zhou L, Wu Y, Machi T, Fudamoto Y, Koshizuka N and Murakami M 2001 *Appl. Phys. Lett.* **79** 1154

[4] Zhao Y, Huang D X, Feng Y, Cheng C H, Machi T, Koshizuka N and Murakami M 2002 *Appl. Phys. Lett.* **80** 1640

[5] Zhao Y, Feng Y, Machi T, Cheng C H, Huang D X, Fudamoto Y, Koshizuka N and Murakami M 2002 *Europhys. Lett.* **57** 437

[6] Wang J, Bugoslavsky Y, Berenov A, Cowey L, Caplin A D, Cohen L F, MacManus Driscoll J L, Cooley L D, Song X and Larbalestier D C 2002 *Appl. Phys. Lett.* **81** 2026

[7] Eorn C B *et al* 2001 *Nature* **411** 558

[8] Chen Q and Yun S 2000 *Mater. Res. Bull.* **35** 1915

[9] Takenobu T, Ito T, Chi D H, Prassides K and Iwasa Y 2001 *Phys. Rev.* B **64** 134513

[10] Mickelson W, Cumings J, Han W Q and Zettl A 2002 *Phys. Rev.* B **65** 052505

[11] Bharathi A, Jemima Balaselvi S, Kalavathi S, Reddy G L N, Sankara Sastry V, Hariharan Y and Radhakrishnan T S 2002 *Physica* C **370** 211

[12] Xu M, Kitazawa H, Takano Y, Ye J, Nishida K, Abe H, Matsushita A, Tsujii N and Kido. G 2001 *Appl. Phys. Lett.* **79** 2779